SUPPLEMENTARY DATA for:

An 'open' structure of the RecOR complex supports ssDNA binding within the core of the complex

Jens Radzimanowski[1,6], François Dehez[2,3], Adam Round[4], Axel Bidon-Chanal[2,3], Sean McSweeney[1], Joanna Timmins[1,5,*]

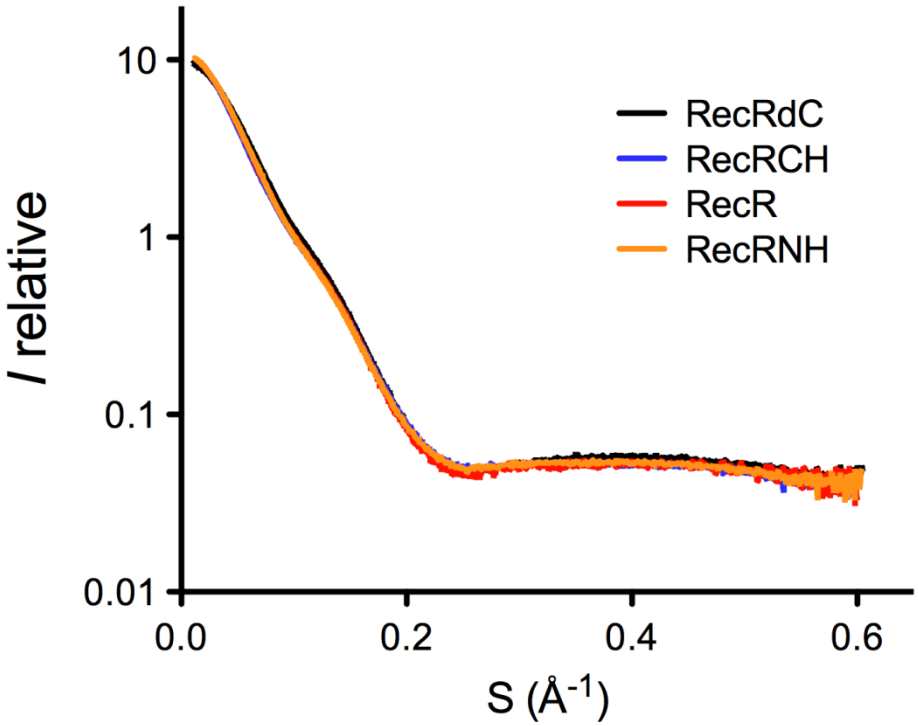

Figure S1: SAXS curves of various RecR constructs. RecRdC (black) comprises residues 1-197, RecR (red) corresponds to full-length RecR with no His-Tag, RecRCH (blue) to full-length RecR with a C-terminal His-Tag and RecRNH (yellow) to full-length RecR with an N-terminal His-Tag.

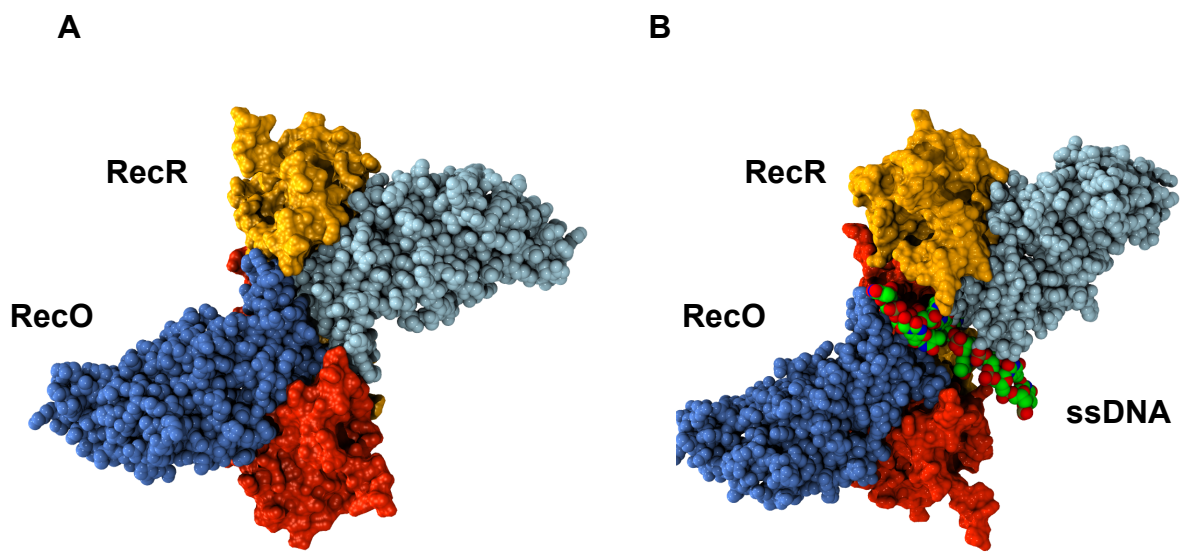

Figure S2: Comparison of the RecOR-'closed' structure (A) with that of the RecOR-'open' structure (B). For clarity, only two RecR molecules are illustrated (in red and yellow) and the two RecO molecules are colored in light and dark blue. In (A), the two RecO molecules interact tightly, whereas in (B) a wide groove is formed between the two RecO molecules and through the RecR tetramer, which could accommodate ssDNA (illustrated as a space-filling model, colored red and green).

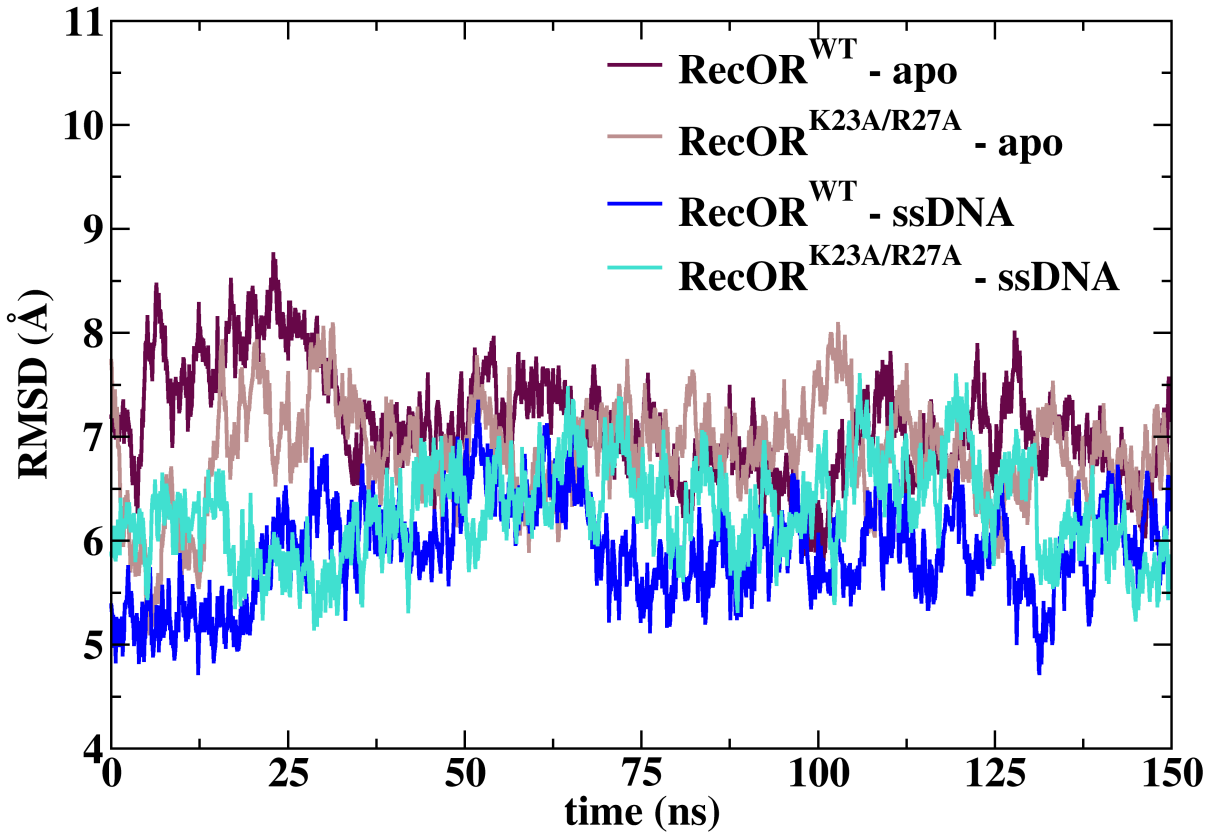

Figure S3: Time evolution of the atom-positional rmsd over the backbone atoms of RecOR in *i*) RecOR wild-type -*apo*, *ii*) RecOR wild-type -ssDNA, *iii*) RecOR$^{K23A/R27A}$ -*apo* and *iv*) RecOR $^{K23A/R27A}$ -ssDNA with respect to the RecOR-'open' crystal structure.

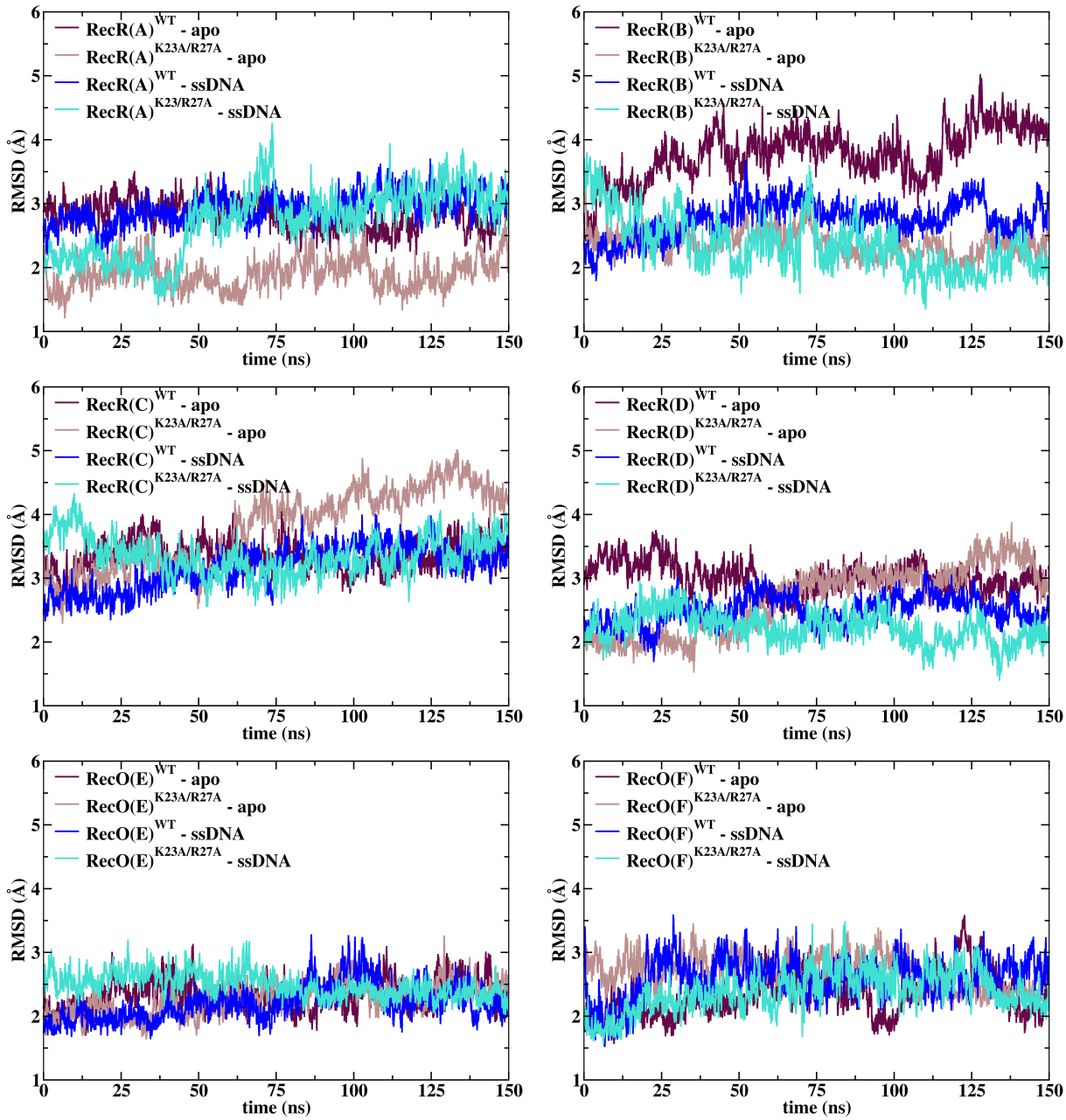

Figure S4: Time evolution of the atom-positional rmsd over the backbone atoms of each RecOR individual protein (chain A,B,C,D of RecR and E,F of RecO) in *i*) RecOR wild-type - *apo*, *ii*) RecOR wild-type- ssDNA, *iii*) RecOR$^{K23A/R27A}$ -*apo* and *iv*) RecOR $^{K23A/R27A}$ -ssDNA with respect to the RecOR-'open' crystal structure.

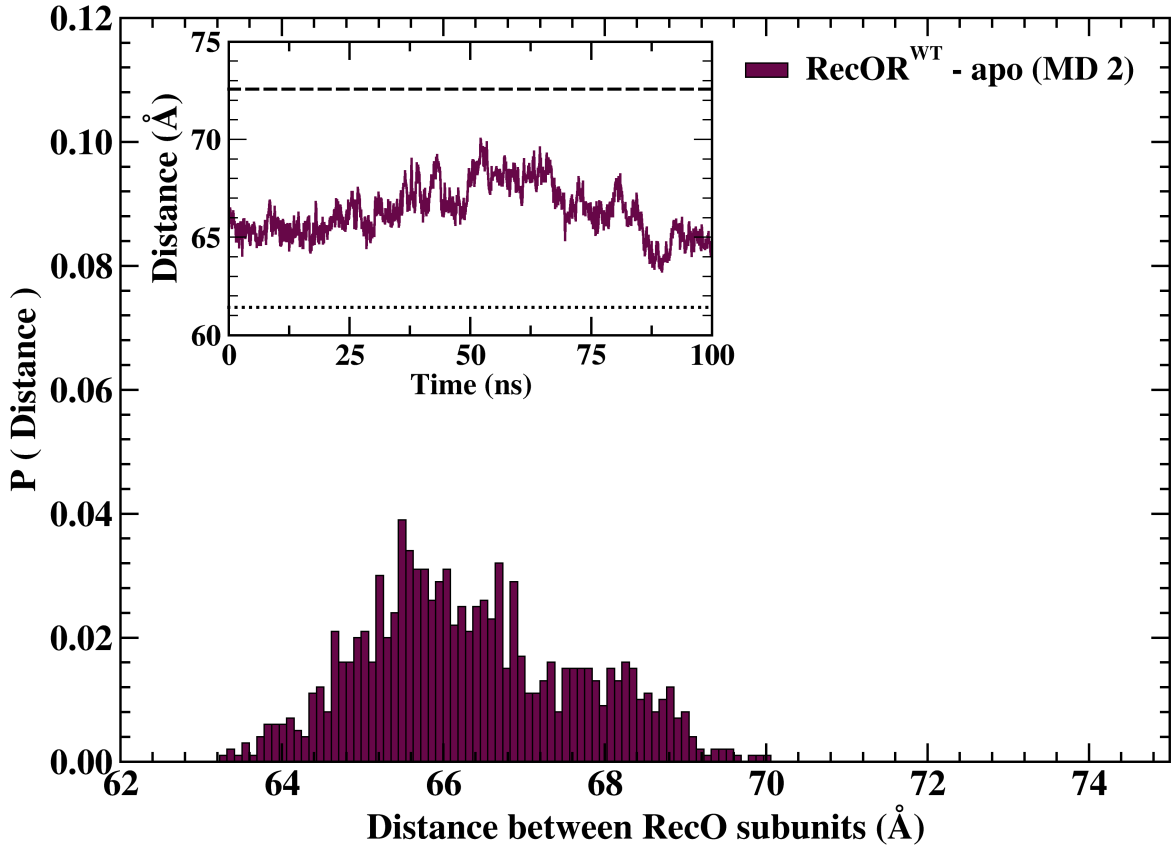

Figure S5: Probability distribution and time evolution (inset) of the distance between the center of mass of the two RecO subunits monitored along an independent 100-ns trajectory of RecOR wild-type-*apo*. Dotted and dashed lines (inset) depict the corresponding distances observed in RecOR-'closed' (61.4 Å) and RecOR-'open' (71.6 Å), respectively.

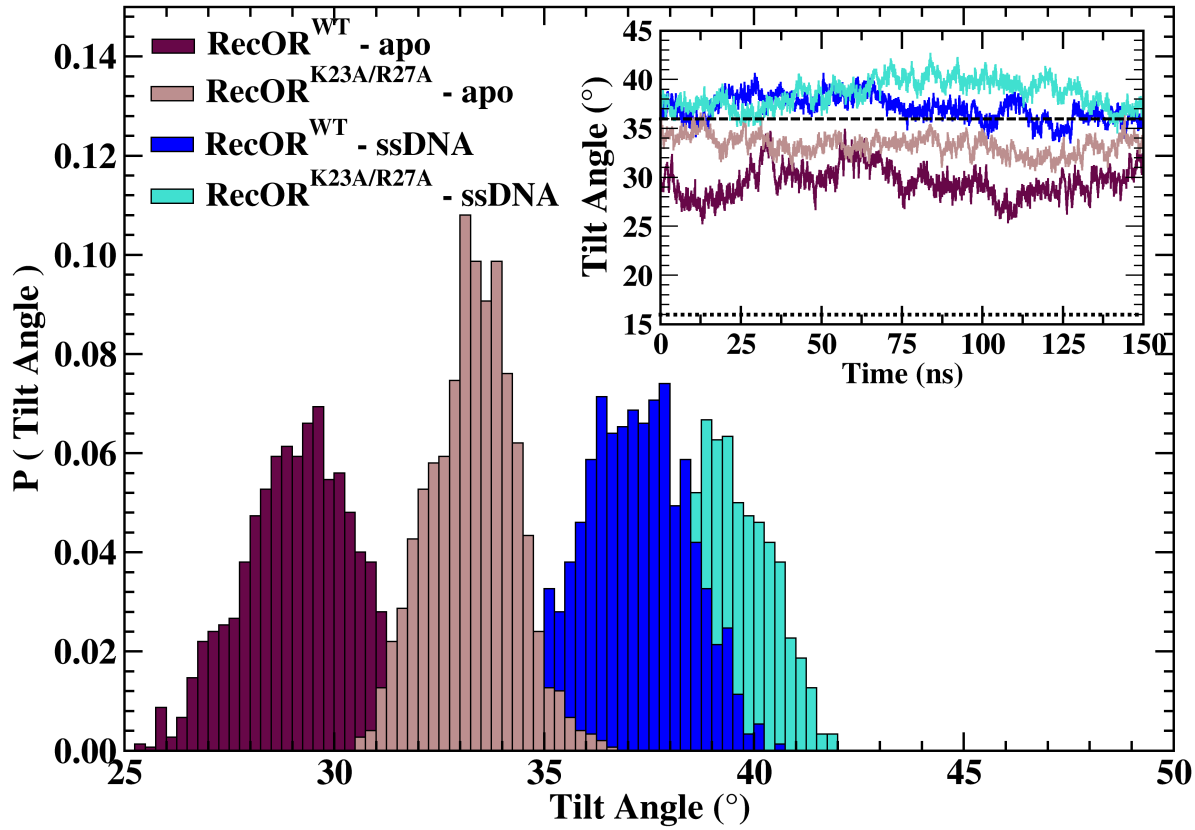

Figure S6: Probability distribution and time evolution (inset) of the tilt angle between the normal to the RecR tetrameric ring and the axis connecting the center of mass of the two RecO subunits in *i*) RecOR wild-type -*apo*, *ii*) RecOR wild-type -ssDNA, *iii*) RecOR$^{K23A/R27A}$ -*apo* and *iv*) RecOR $^{K23A/R27A}$ -ssDNA. Dotted and dashed lines (inset) depict the corresponding angles observed in RecOR-'closed' (16°) and RecOR-'open' (36°), respectively.

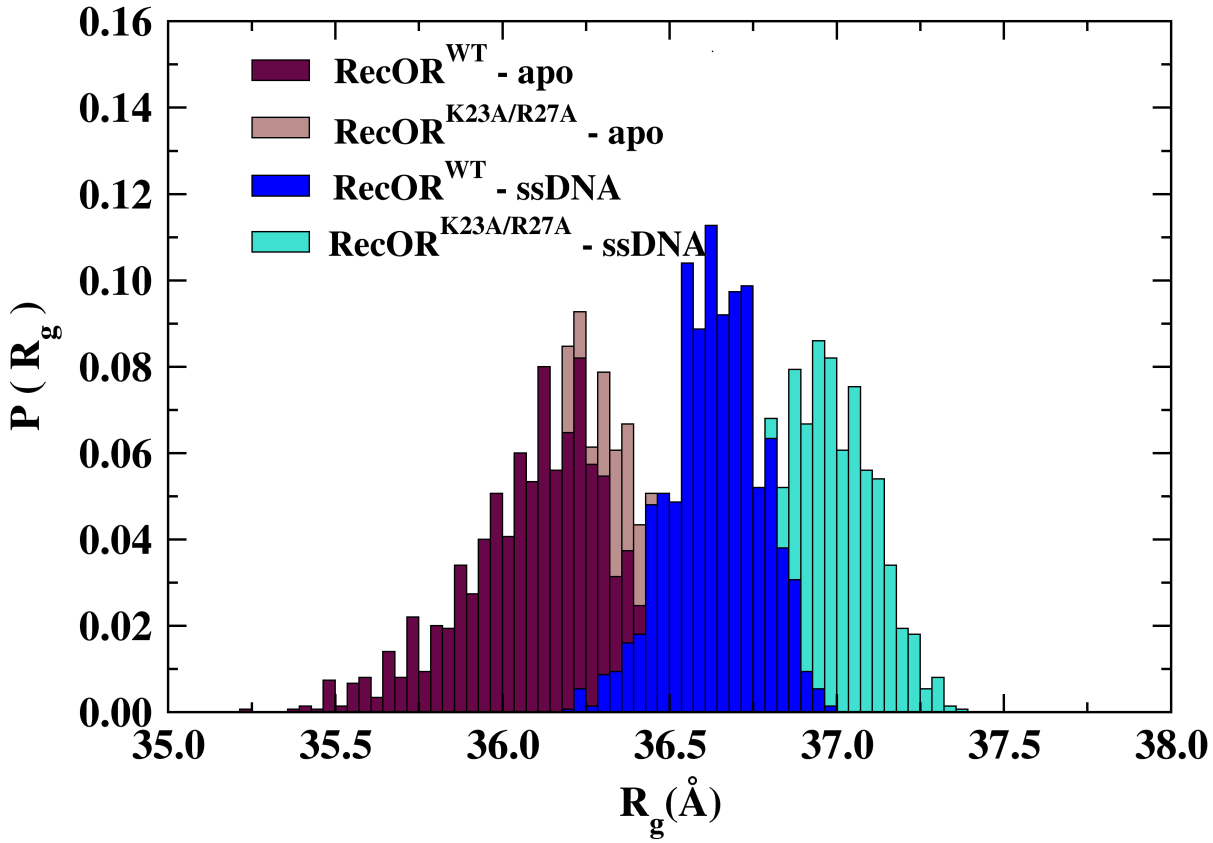

Figure S7: Probability distribution of R_g obtained from the fit of SANS curves against 1.500 complex structures taken all along the 150 ns production runs for *i*) RecOR wild-type - *apo*, *ii*) RecOR wild-type - ssDNA, *iii*) $RecOR^{K23A/R27A}$ - *apo* and *iv*) $RecOR^{K23A/R27A}$ – ssDNA.

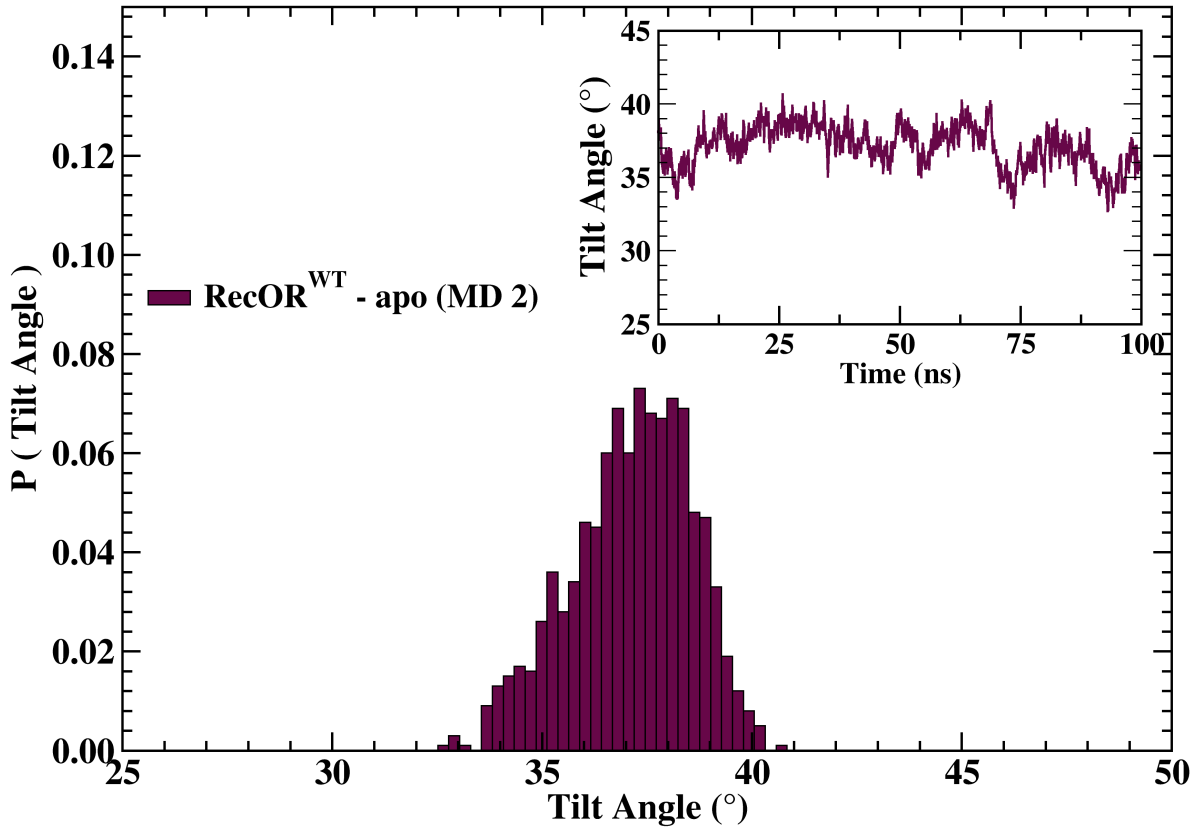

Figure S8: Probability distribution and time evolution (inset) of the tilt angle between the normal to the RecR tetrameric ring and the axis connecting the center of mass of the two RecO subunits monitored along an independent 100-ns trajectory of RecOR wild-type - *apo*.

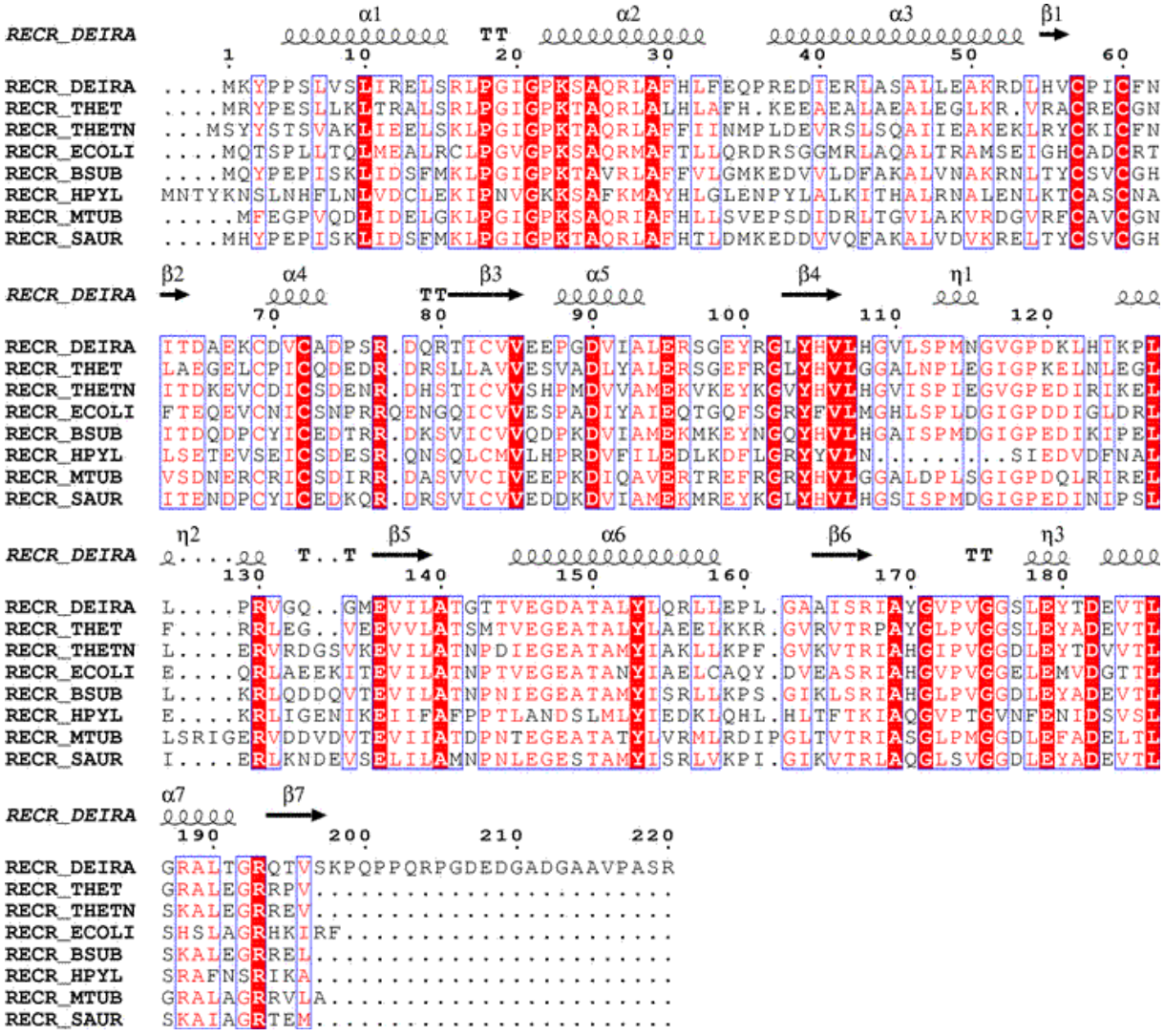

Figure S9: Sequence alignment of RecR proteins from *D. radiodurans, Thermus thermophilus, Thermoanaerobacter tengcongensis, Escherichia coli, Bacillus subtilis, Helicobacter pylori, Mycobacterium tuberculosis and Staphylococcus aureus*. The secondary structure elements of drRecR are shown above the sequences. The alignment was prepared with ClustalW (65) and rendered with ESPript (66).

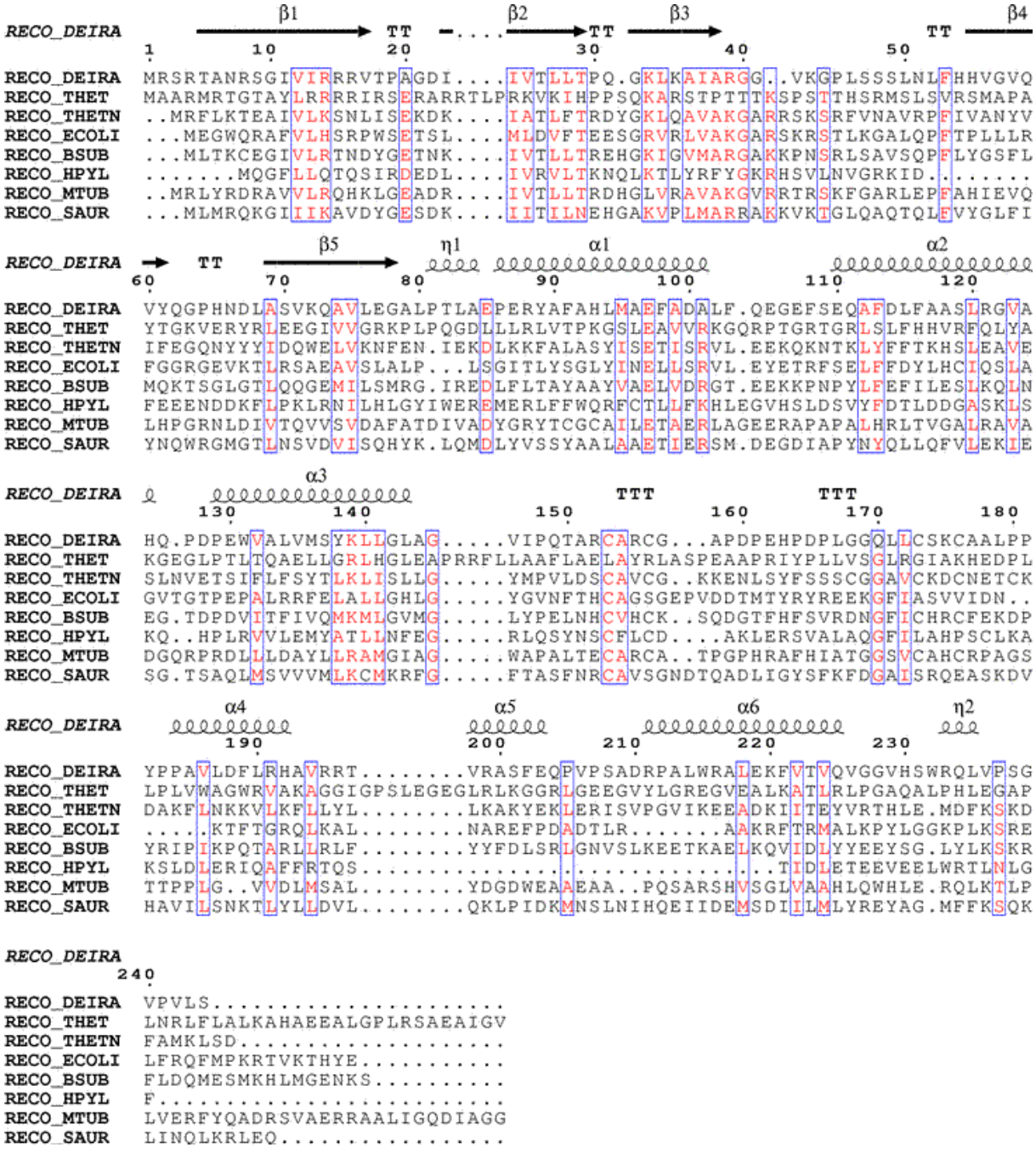

Figure S10: Sequence alignment of RecO proteins from *D. radiodurans, Thermus thermophilus, Thermoanaerobacter tengcongensis, Escherichia coli, Bacillus subtilis, Helicobacter pylori, Mycobacterium tuberculosis and Staphylococcus aureus*. The secondary structure elements of drRecO are shown above the sequences. The alignment was prepared with ClustalW (65) and rendered with ESPript (66).

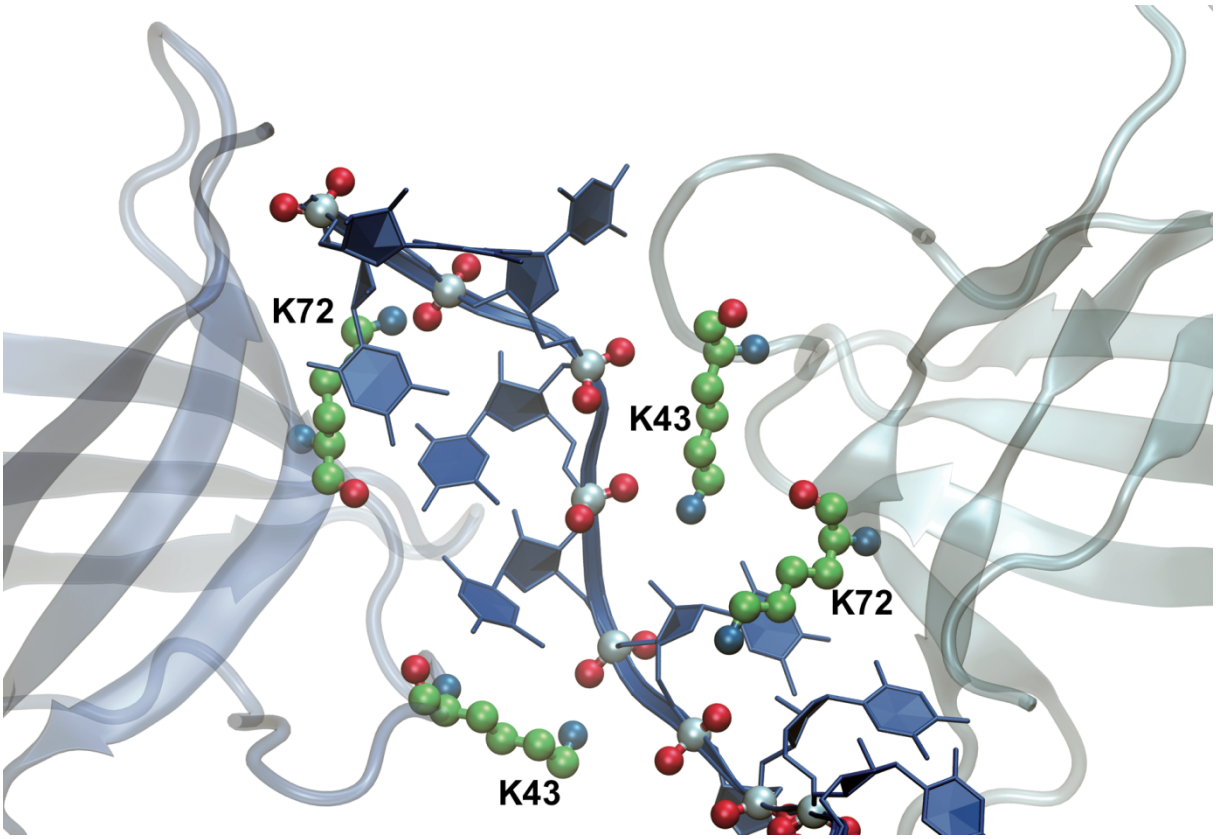

Figure S11: Non-specific recognition of ssDNA by RecOR. Close-up view of the binding of ssDNA to RecO predicted by molecular dynamics, involving electrostatic interactions between lysine residues from the two RecO subunits and phosphate groups from the DNA backbone.